BioScience AFM – Capturing Dynamics from Single Molecules to Living Cells

Dimitar R. Stamov,[1] Stefan B. Kaemmer,[2]* Anne Hermsdörfer,[1] Jörg Barner,[1] Torsten Jähnke,[1] and Heiko Haschke[1]

[1]JPK Instruments AG, Colditzstr. 34-36, 12099 Berlin, Germany

[2]JPK Instruments USA, 4189 Carpinteria Ave., Suite 1, Carpinteria, CA 93013

*stefan.kaemmer@jpk.com

Introduction

The last three decades have seen the rise of the atomic force microscope (AFM) as an indispensable tool for high-resolution structural analysis of specimens ranging from single molecules [1] to complex biological systems such as proteins and cells [2]. Unlike other high-resolution imaging techniques, such as advanced electron microscopy and super-resolution light microscopy, AFM remains the only tool that currently offers premium resolution of the analyzed biological systems while being able to simultaneously acquire information about the sample's mechanical properties at near physiological/native sample conditions. An additional benefit of AFM is that by default it also does not demand any sample modification and therefore does not introduce preparation artifacts.

The two most commonly used AFM modes for investigating biological samples in a near-native environment employ either dynamic or static AFM tip motion (see Figure 1). The dynamic modes, in which a vibrating cantilever is driven over a surface with a defined amplitude, are preferred for soft biosamples because of the less invasive nature of the imaging. Even though repulsive forces are commonly used, resonance dynamic modes generally apply lower forces to the specimen during the imaging process. Pure non-contact techniques are less frequently used with biological samples because of the rather complex composition of the imaging buffers and media used.

Studying single macromolecule dynamics and the function of complex biological systems, such as individual living cells, requires a tool that can provide both high spatial and high temporal resolution [3]. Developments in the last 10–15 years have paved the way toward the application of ultra-small cantilevers, piezoactuator-based sample scanners, and optical beam deflection (OBD) detectors for studying high-speed single-molecule processes [4–6]. Such high-speed developments are rarely applicable for living cells as they exhibit a significantly reduced *xy*-scan window of only a few microns and a *z*-range of less than a micrometer [7]. Recent developments in fast tip-scanning AFMs [8] allow the successful structural analysis of a number of dynamic processes in cells such as exocytosis, vesicle transport, cytoskeleton reorganization, and cell migration, all taking place on the timescale of seconds. Structurally resolving morphological surface changes and the above-mentioned cellular events are no longer limited by the fundamental diffraction limit inherent to conventional light microscopy. It is the combination of light microscopy and AFM that leverages the advantages of optical/fluorescence detection systems enabling truly correlative AFM [9]. This article describes some examples of these techniques.

Materials and Methods

Combining light optical microscopy and AFM. Combining AFM with optical information has become a standard when working with biological samples above Abbe's resolution limit, as well as with single molecules carrying immunolabels. The convenience of combining high-resolution AFM information from an optically

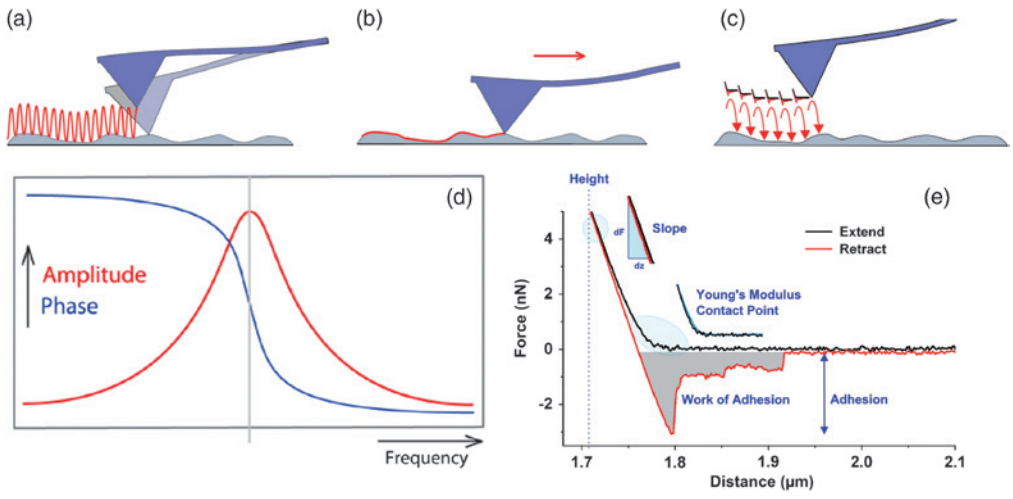

Figure 1: Conventional AFM imaging modes. (a) The most commonly used dynamic AFM mode is AC in which a cantilever is oscillated with a certain amplitude close to its resonance frequency and intermittently touches the surface. (b) Static AFM imaging (contact mode) maintains a constant deflection of the cantilever (pre-set force) to the sample while raster scanning and without detaching from the surface. (c) Quantitative imaging allows recording of a complete force curve (vertical application of a pre-set force in approach/retract regime) at each pixel. (d) Further monitoring of amplitude damping or phase shift during AC imaging enables related amplitude and phase modulation modes. (e) Simultaneous acquisition of the cantilever-sample interaction during the force spectroscopy-based QI mode enables height determination, adhesion, or mechanical characterization.

https://doi.org/10.1017/S1551929515001005 Published online by Cambridge University Press

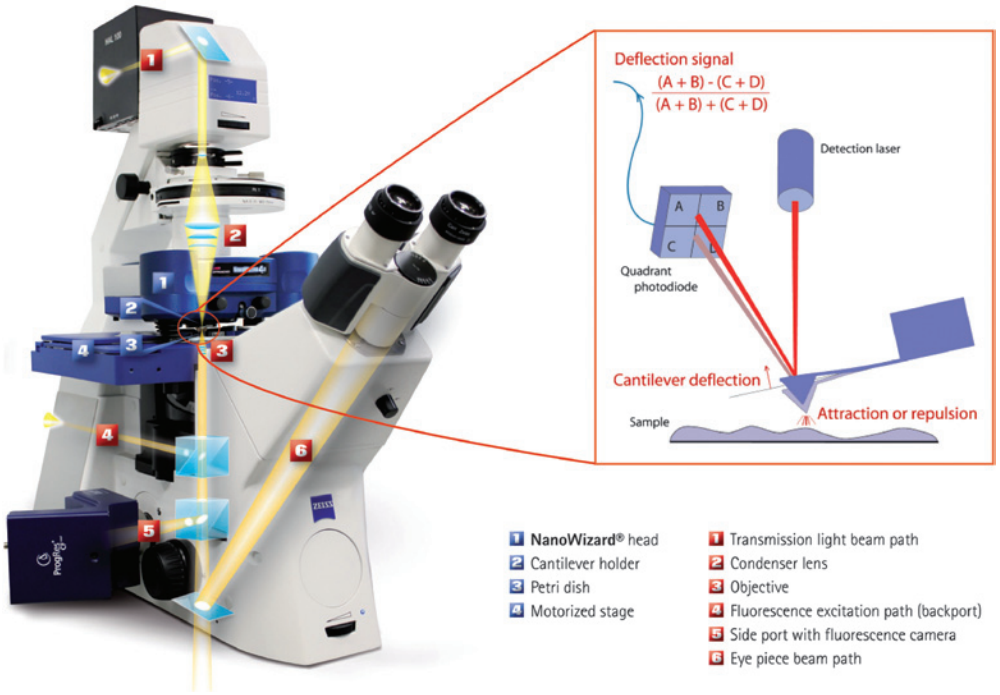

Figure 2: Setup of a tip-scanning AFM with an inverted optical microscope. The AFM head is placed on a motorized stage carrying a Petri dish holder for environmental temperature control and maintenance of living cells. Use of light optics is made possible by the transparent central part of the AFM head. The inset on the right depicts the basic optical lever principle of AFM detection in which cantilever deflections are transferred to a four-quadrant photodetector. The AFM head (NanoWizard® 4a/JPK Instruments), is placed on an inverted light optical microscope (AxioObserver/Zeiss) equipped with a side-port fluorescent camera (ProgRes®/Jenoptik).

transparent sample with condenser optics in an inverted optical microscope (IOM) is demonstrated in Figure 2. The choice of a tip scanner design is crucial for applications where the optical image of the specimen needs to remain in focus during AFM measurements. The transparent central area of the AFM head is the only practical design that would allow the combination of top view optical access and simultaneous AFM. The piezo-scanner has a flexure mechanism that decouples the *xy*-axes of motion from the *z*-scanner. This is particularly important for high-resolution applications and data reproducibility.

Co-localization of all datasets. To make sure that structural and optical information can be truly correlated, it is important to remove any distortions arising from lens aberrations and non-linear alignment of mirrors in the optics system. Optical artifacts such as non-linear stretching, rotating, and off-setting of light microscope images are present in nearly all types of optical setups. By taking advantage of the accuracy of the closed-loop AFM, JPK's DirectOverlay™ feature is able to correct for any lens imperfections and transfer the optical image to the calibrated AFM coordinate system. An immediate benefit is the possibility to carry out all measurements directly by choosing locations from within the optical image. An example is given with a super-resolution direct stochastic optical reconstruction microscopy (dSTORM) setup and Alexa-647-labeled microtubules in HeLa cells (Figure 3).

In addition to the accurate overlay of light optical and AFM information, the integration of both signals substantially reduces the total imaging time by avoiding the necessity of rescanning AFM areas, thereby reducing physical phenomena such as tip-contamination and the wearing of functionalized tips used for molecular recognition.

Fast Scanning. The application of conventional AFM imaging for imaging of soft samples (particularly in liquid) is fundamentally limited to the use of very low imaging rates. This is due to the rather slow feedback of the available setups. Consequently, dynamic processes taking place at the second and even millisecond scale are impossible to capture. There is a range of developments made over the last two decades that make fast imaging possible. The main improvements are a larger feedback bandwidth, high-resonance *z*-scanners, and thermally quieter cantilevers [4, 6, 10]. The higher oscillation frequencies of the cantilever, larger feedback bandwidth, and enhanced *xy*-movement allow increased speed of the cantilever without decreasing the resolution of the measurement or damaging very sensitive samples.

Quantitative Imaging™ (QI). : QI curve is a force-distance curve based combined imaging and spectroscopy mode ensuring that not more than a set maximum force is applied to the sample (Figures 1c and 1e) at each imaging location (pixel). Storing the entire force curve behind every pixel enables dedicated operations allowing extraction of quantitative data from QI images or maps. The QI software employs the acquired data to calculate the properties in question, using either already-available or a customized-fit algorithm. Typical parameters that can be extracted are work of adhesion, the actual adhesion, and contact point determination. Specific adhesion events can be detected, and Young's modulus can be calculated using different contact mechanics models. Furthermore, the contact point height determination enables the possibility of creating the so called zero-force image (having no indentation), as well as examining the topography and indentation information from the sample at different forces within the range of the applied setpoint. This enables 3D tomographical reconstruction of the sample at a later stage and correlation of the information coming from different channels.

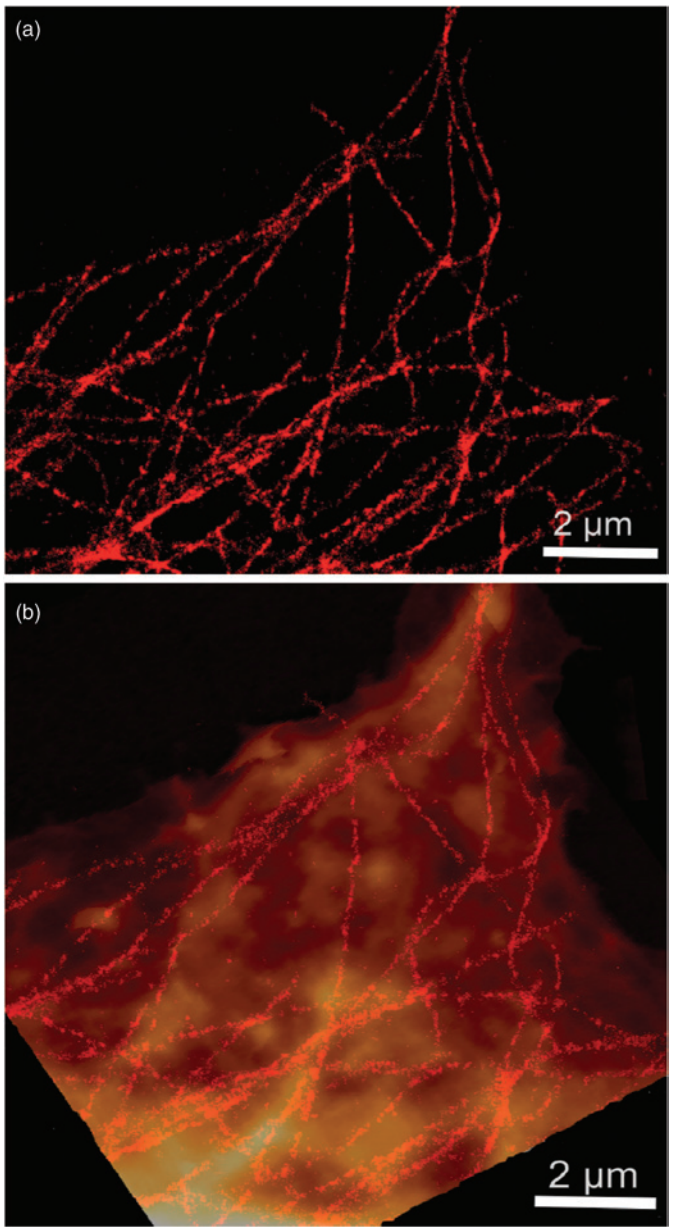

Figure 3: Proper integration of AFM and inverted optical microscope allows accurate co-localization of all datasets. Microtubules in HeLa cells (a) labeled with Alexa-647 antibodies in buffer solution from direct stochastic optical reconstruction microscopy (dSTORM). (b) Overlay of AFM surface data and the dSTORM image allows the correlation of cell membrane surface texture (from AFM) and the positions of the microtubules (from dSTORM). The *z*-scale of the AFM image is 400 nm.

Results

Submolecular structure of soft biological molecules. Specimens for AFM work, and particularly biosamples, are often analyzed at near-room or slightly elevated temperatures. All AFM systems are prone to drift caused by different thermal expansion of the construction materials used and thus are susceptible to external environmental heat dissipation [11]. Unlike conventional configurations that require long scanning times of at least a few minutes, the application of fast-scanning AFM mitigates this problem, which is of particular importance in the case of very sensitive and quickly deteriorating samples.

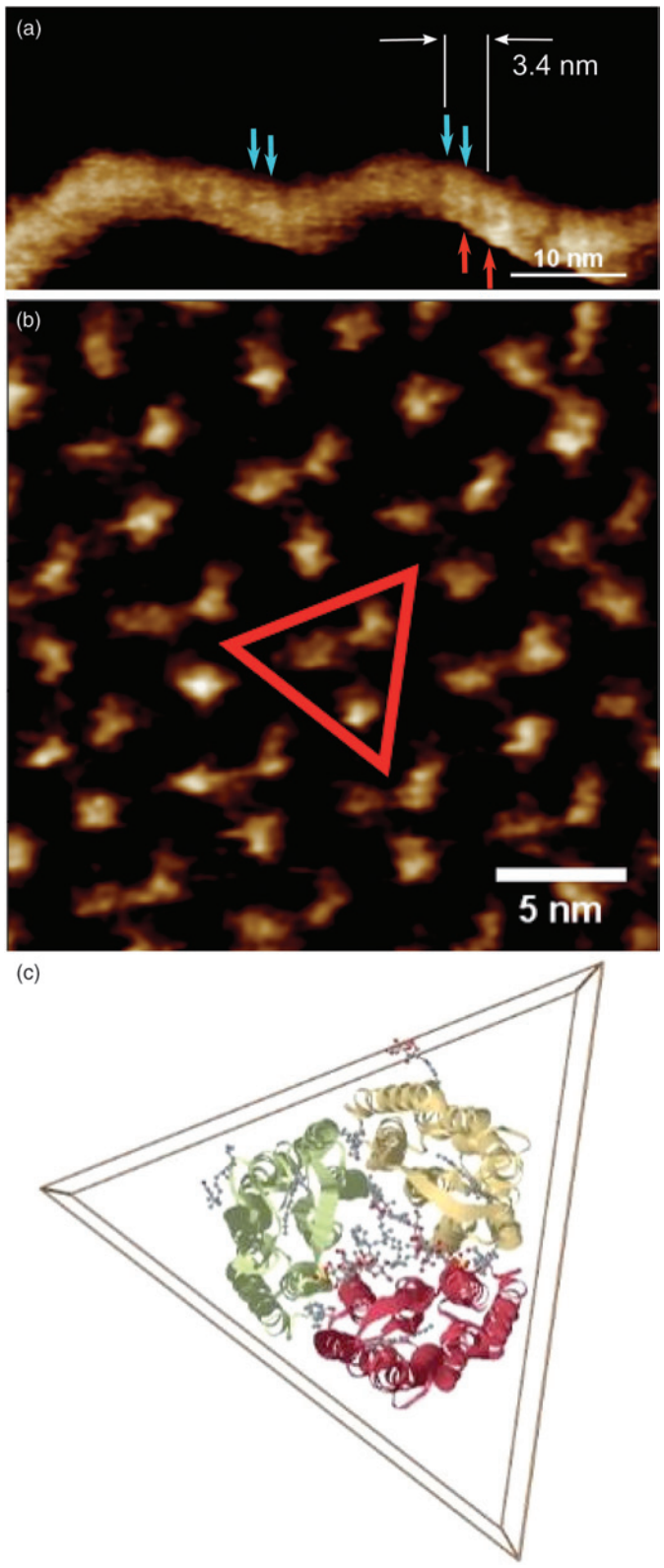

Figure 4: Fast-scanning AFM. (a) AFM image of lambda phage DNA recorded at 15 Hz line rate showing the major (labeled with red) and minor grooves (shown here in blue) in the double-helical repeat of 3.4 nm. (b) The subtrimeric structure of bacteriorhodopsin can be visualized using a line rate of 30 Hz in 10 mM TRIS (150 mM KCl) buffer. (c) A 3D view of a "1BRR" PDB trimer/lipid complex from www.rcsb.org given for comparation. The z-scales in (a) and (b) are 3 nm and 0.4 nm, respectively.

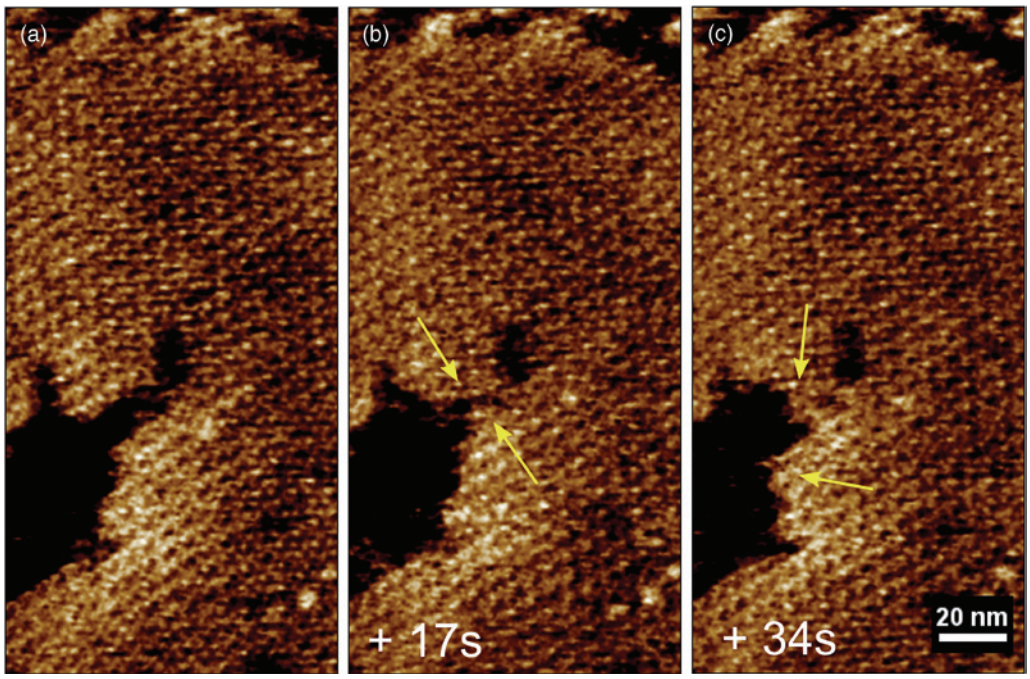

Figure 5: Lateral membrane patch dynamics of bacteriorhodopsin. Addition and dissociation of trimers at the periphery of a membrane patch (relative differences between frames shown with yellow arrows) observed with fast-scanning AFM at time intervals of 17 seconds. The images are crops of the original 512×512 pixel-frames recorded at a line rate of 30 Hz. The *z*-scale in (a–c) is 1 nm.

Figure 4a shows an example with a soft lambda phage DNA molecule imaged in buffer solution. The double helix of DNA is typically revealed by applying a force range between 50–100 pN [12]. Crystallographic data give the size of the 2 nm thick DNA double helix, with one whole revolution around its axis of 3.4 nm, comprised of a major groove (2.2 nm, see Figure 4a, red arrows) and a minor groove (1.2 nm, see Figure 4a, blue arrows). The DNA data obtained by AFM in solution are in very good agreement with the one from crystallographic measurements reported in literature.

Another example is the high-resolution imaging of bacteriorhodopsin (BR). Arranged as a 2D protein crystal of trimeric polypeptide molecules consisting of seven transmembrane alpha helices each, BR functions as a light-driven proton pump (Figure 4b). The vast majority of previous high-resolution conventional AFM scans of this molecule reported in the literature were almost exclusively done with static mode imaging [13]. The application of fast scanning shown allows AFM to get structural information that is comparable to the details coming from crystallographic data (Figure 4c). There was no need to average several data sets.

Dynamic changes in proteins. Fast-scanning AFM allows the imaging of soft samples in liquid. It is now possible to visualize a range of dynamic processes taking place on the scale of seconds and milliseconds with adequate spatial resolution. Figure 5 shows another example with BR, a light-driven proton pump found in some purple membrane-containing *Halobacterium* species. By using fast scanning with a line rate of 30 Hz, it is possible to visualize the membrane patch fluidity. In particular, the images depicted in Figure 5 reveal the addition and removal of BR trimers without introducing scanning defects/ artifacts into the patch.

The newly bound and dissociated BR molecules can be identified in groups of trimers between the individual frames. This is mostly because the temporal resolution of lateral bond lifetime of such individual events is typically on the timescale of a few hundred milliseconds to a few seconds, which is much less than the time separation of 17 s of the original frames shown.

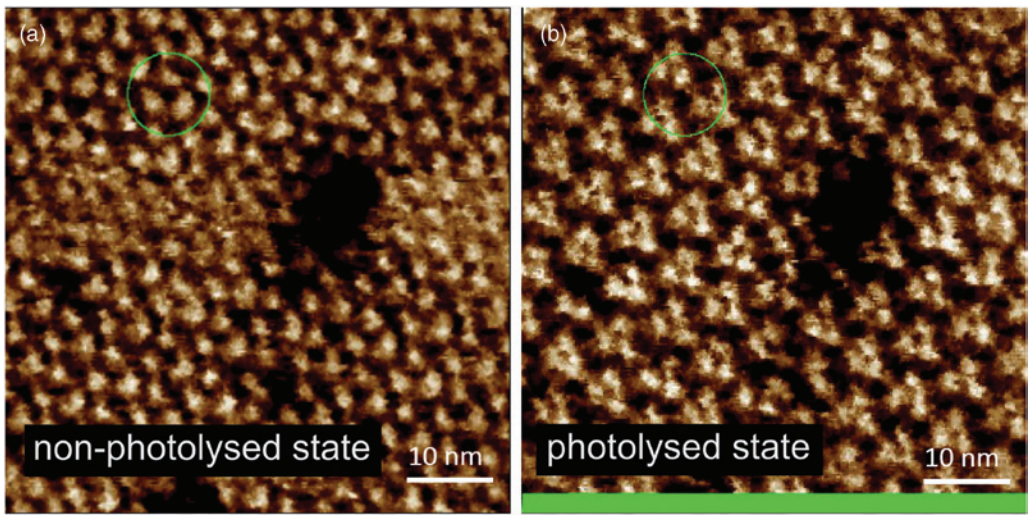

Figure 6: Photodynamic cycle changes in bacteriorhodopsin. Frames of (a) non-photolyzed and (b) photolyzed states of BR in a membrane patch as a part of the reversible photoactivation series. The light-illumination part of the cycle is designated with green at the bottom of (b). Upon switching the green light off, the BR molecules revert back to their non-photolyzed-state conformation over a period of seconds. The outlined sector in (a) and (b) shows the associated structural change (displacement of the monomers with respect to the trimeric center of about 0.7 nm). (a) and (b) were recorded at a line rate of 32 Hz. The *z*-scale is 0.8 nm.

Conformational change in molecules. Fast scanning allows study of the photocycle kinetics of the BR molecule. The BR molecule is light-sensitive

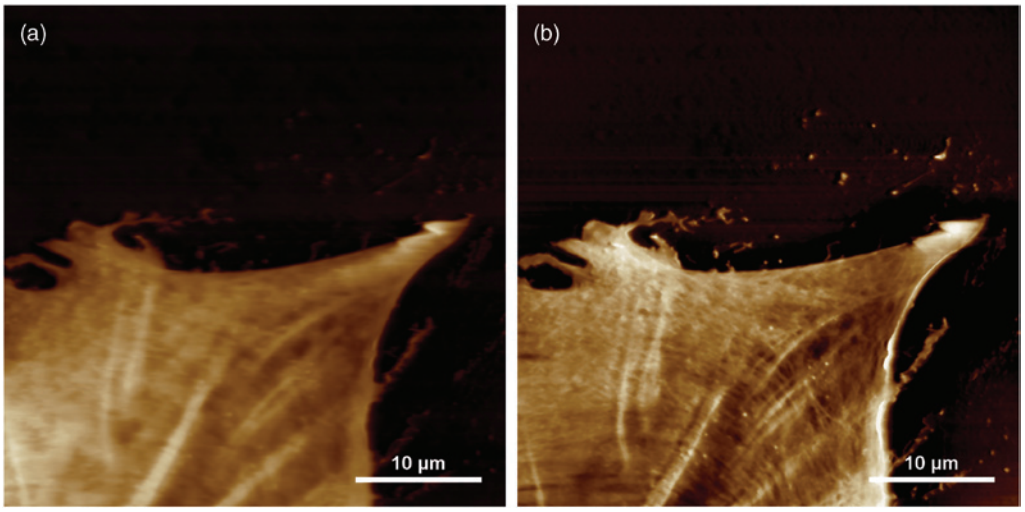

Figure 7: AFM image of the cytoskeleton structure of a KPG7 fibroblast. (a) Height and corresponding (b) phase channel from a scan of living cells cultured at 37°C in a Petri dish heater recorded at a line rate of 6 Hz. The recording of the cytoskeleton filaments with such a high contrast at a cantilever velocity of 600 µm/s is possible with fast-scanning AFM. *Z*-scales in (a) and (b) are 300 nm and 10 degrees, respectively.

where each monomeric bundle of seven alpha helices packs a pigment molecule called retinal [14]. Upon absorption of a photon, the chromophore undergoes an all-trans to 13-cis conformational change, which triggers a proton flow directionality and a cascade of changes in the BR structure. In wild-type BR, this process is extremely quick (10 ms), but the existence of point-mutations in specific BR types substantially inhibits their response to light. In particular, the D96N mutant BR carries an Asp96 point mutation to Asn, which slows down one of the longest intermediates of the phototocycle (M) in the mutant compared to the wild type protein by about 50 times [15]. The two recurring frames in Figures 6a and 6b depict the structural/conformational differences in the BR trimers between their photolyzed (Figure 6b) and non-photolyzed state (Figure 6a). As seen from the outlined sector in Figures 6a and 6b, the structural change is associated with an outward displacement of the monomers with respect to the trimeric center (approximately 0.7 nm) and is rotated counterclockwise.

Morphological changes in living cells. Conventional AFM imaging of live cells in dynamic (and static) mode is challenging because of the rather long image acquisition times and the relatively slow feedback being unable to cope with the soft and topographically inhomogeneous samples. Fast-scanning AFM can now be applied for study of weak and rapidly changing signals such as dynamic cellular processes at near-physiological conditions. Figures 7a and 7b highlight a 1024-pixel 40 µm scan of a living KPG7 fibroblast recorded in DMEM/F-12 cell culture medium imaged at 37°C. The filamentous structure of the underlying transverse and radial cytoskeletal arcs is immediately resolved. The cell was imaged for a few hours at different speeds and scan sizes to verify that the tip-sample interaction is not leading to a specific cell retraction or introduction of further morphological artifacts.

The direct observation of cell membrane dynamics is another example discussed. Living cells are constantly interacting with their surroundings by exchanging molecules and signals. Membrane ruffling or vesiculation of external molecules and vesicles (endocytosis), release of metabolitic degradation products, and release of signaling molecules to other cells (exocytosis) are mostly associated with membrane turnover. The timescale of most of these processes can depend on the type of membrane fusion or secretion and normally ranges from seconds to minutes [16, 17]. The example below shows a plausible exocytosis event on the timescale of 30–40 seconds, which is associated with a morphological change happening directly on the cell surface (Figures 8a–e).

The budding vesicle can be clearly resolved in AFM phase images because of the much higher sensitivity of the phase channel to the rapidly changing and weak signals from the morphological differences in the cell surface. The same features are resolved in the height channel as well, corresponding to a gradual increase of the height of the budding area from 10 to about 25 nm.

Dynamic AFM modes. The most commonly used dynamic AFM mode is amplitude modulation AFM

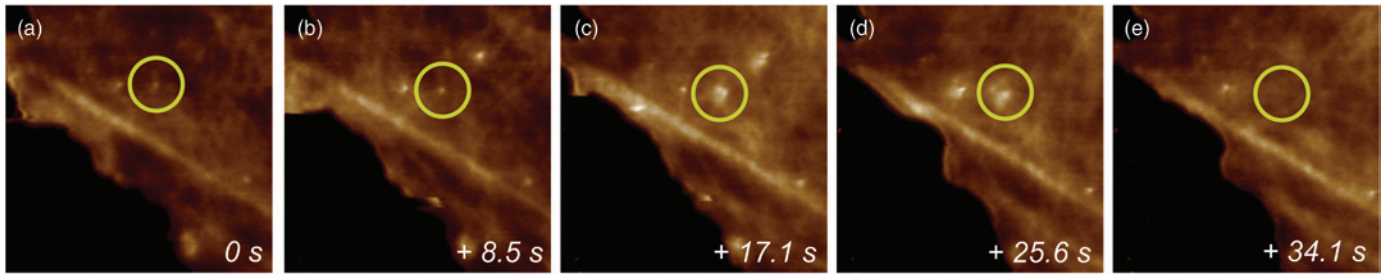

Figure 8: Fast scanning of surface dynamics of KPG7 fibroblasts with high spatiotemporal resolution (a–e). Phase images acquired with a temporal resolution of ~8.5 s per frame. Yellow circles emphasize the budding event discussed in the main text. Scans in (a) through (e) contained 256 × 256 pixels per frame and were acquired at a line rate of 30 Hz. Image width = 5 µm.

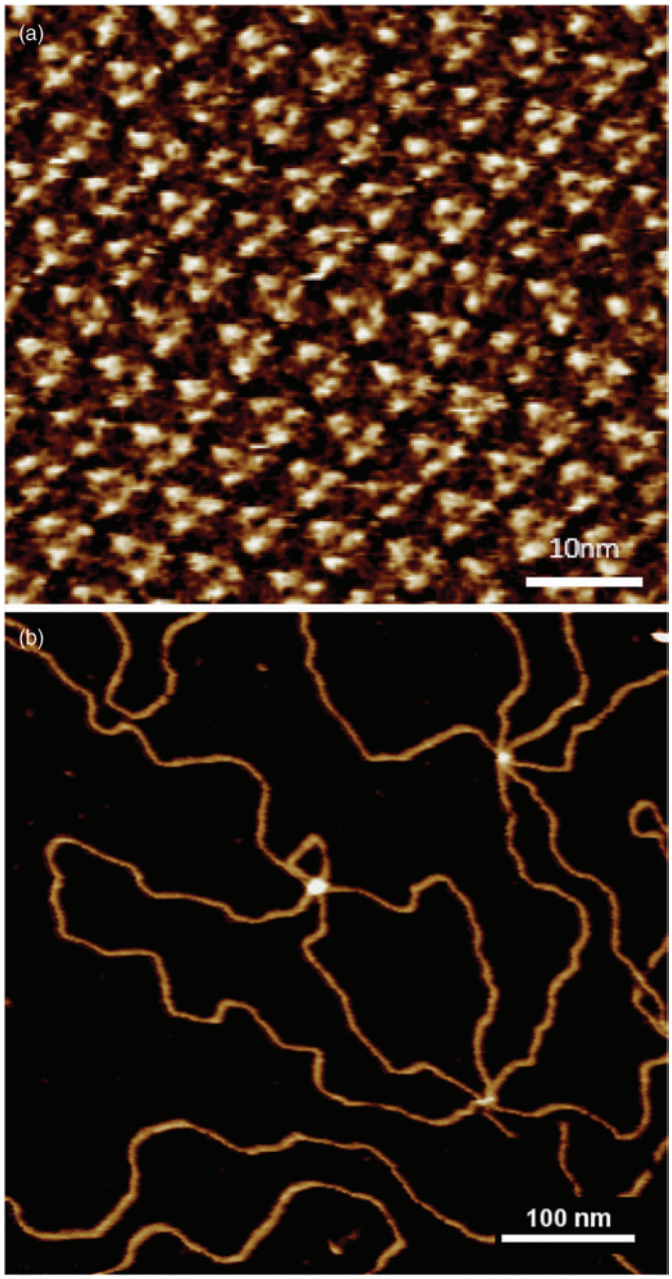

Figure 9: Phase-modulation AFM of biomolecules in buffer. (a) Phase-modulation height image of bacteriorhodopsin in 10 mM TRIS (150 mM KCl) buffer. (b) Height channel from a phase-modulation scan combined with fast scanning on lambda phage DNA sample in 10 mM HEPES (2 mM Ni^{2+}) buffer, acquired at a line rate of 10 Hz. *Z*-scales in (a) and (b) are 0.4 and 4 nm, respectively.

(AM-AFM). In AM-AFM, the cantilever is excited with a fixed amplitude and frequency around its resonance with the tip-sample interaction forces being detected as an amplitude damping [18]. It has been shown, however, that phase response in phase modulation AFM (PM-AFM) is much faster compared to AM-AFM. This in turn allows for excellent force control in addition to the application of really small cantilever amplitudes of often 0.1–0.2 nm to minimize tip-sample interaction. This makes PM-AFM the preferred dynamic AFM mode for high-resolution imaging of small samples like soft biomolecules in liquid where precise tip-sample force control is essential. Figure 9 shows examples of this mode from the previously described purple membrane protein bacteriorhodopsin and a soft lambda phage DNA.

Force-controlled AFM. Traditional AFM imaging modes, in particular contact mode, have some well-known drawbacks for challenging samples that exhibit steep edges or are simply too soft, sticky, or loosely attached to the surface. These problems originate from the relatively high lateral/shear forces that are typically applied with very rough or heterogeneous samples and may result in distortion of some sample features. Some of these effects are overcome in dynamic AM-AFM with the trade-off of sometimes lower resolution.

QI mode solves this problem by virtually eliminating all lateral forces and simultaneously allowing the user to directly control the force applied at every pixel of the image. The QI method is a force-distance-curve-based AFM mode ensuring that not more than a user set force is applied to the sample. A novel tip movement algorithm records a complete force curve at every pixel while only performing lateral movement between pixels. The QI mode produces a complete map with a high spatial resolution recorded with an imaging speed of a few minutes using a linear velocity movement of the cantilever within the entire force curve. This opens many possibilities for real force curve analysis and extraction of various material properties. An example of such a force curve and the parameters that can be extracted from it is given in Figure 1e.

Acquiring an entire force-distance curve at every pixel enables several operations for extraction of quantitative data. The acquired data can be used to calculate the nano-mechanical properties using either standard or customized-fit algorithms. Typical parameters that can be extracted include the work of adhesion, the actual adhesion, and contact point determination. Specific adhesion events can be detected and Young's modulus can be calculated using an appropriate contact mechanics model. The contact point height determination enables the recreation of the so-called zero-force image (having no indentation) or simply the topography and indentation information from the sample at different forces within the range of the applied set point (Figures 10a and 10b). The high sensitivity and versatility of this method becomes even more obvious when applied to single molecules. This is illustrated with the resolution of the subtrimeric structure of the purple membrane protein bacteriorhodopsin (Figures 10c–e). A single measurement set shows the differences in sample topography at three different forces and allows the user to adapt the measurement settings in real time. This also enables the 3D tomographic reconstruction of the sample at a later stage and the correlation of the information coming from different channels.

Conclusions

Biological AFM has come a long way since the invention of the scanning probe technique in 1986. The

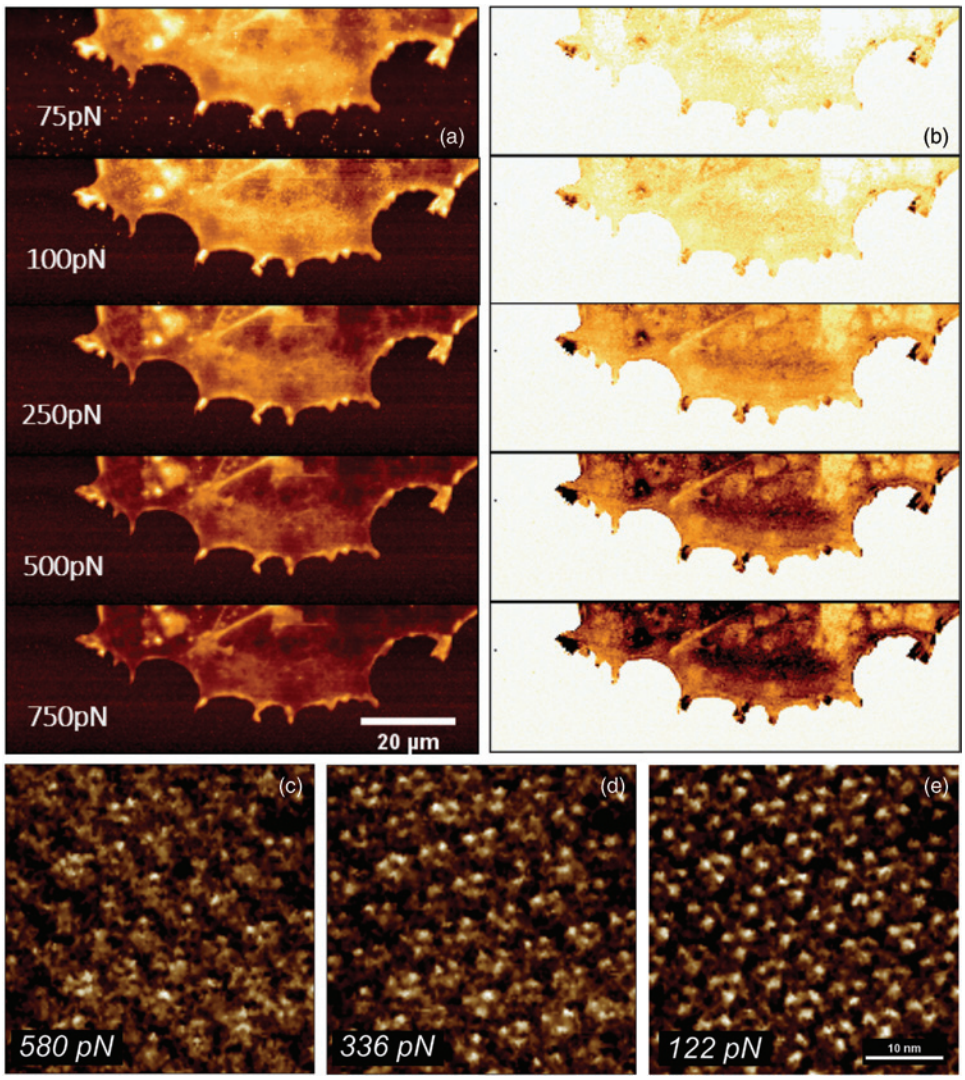

Figure 10: Quantitative Imaging™ of biological samples. Recording a complete force curve at each pixel with a pre-set vertical force eliminates lateral tip-sample forces. (a) An example with a very soft COS7 cell line with a low expression level of cytoskeletal filaments. The complete set of recorded force curves unlocks a number of possibilities for offline analysis as demonstrated by the set-point height/topography (a) and sample indentation (b) at different forces. The online reconstruction of the set-point height at different forces allows either optimal resolution or nano-deformation of the sample, shown here with bacteriorhodopsin in buffer (c–e). *Z*-ranges in (a), (b), and (c–e) are 0–800 nm, 400–0 nm, and 0–600 pm, respectively.

SPM instruments today offer full integration with inverted light optical microscopes, giving researchers the flexibility of utilizing the benefits of both techniques in simultaneously acquired datasets. The integration with super-resolution microscopy pushes the boundaries even further by merging AFM and light optical microscopy into a seamless measuring system. The availability of specialized imaging modes helps to unravel structural problems that were not addressable by the AFMs of a decade ago. Finally, the emergence of fast-scanning AFM in combination with inverted light microscopy in a form that is directly applicable to life science research helps to get a more detailed understanding of dynamic processes in biology.

Acknowledgements

We would like to thank Josef Madl and Winfried Römer (BIOSS, Freiburg, Germany) for kindly providing the HeLa samples used for Figure 3. The bacteriorhodopsin sample used for Figures 4b, 5a–c, 9a, and 10c–e was contributed by the group of Daniel J. Müller (ETH Zürich, BSSE Basel, Switzerland). The D96N mutant sample was supplied by Patrick Bosshart (Basel, Switzerland). The living cells used for measurements in Figures 7, 8, and 10a–b were generously provided by the group of Andreas Herrmann (Humboldt University, Berlin, Germany). The authors would like to thank Tanja Neumann and Florian Kumpfe (JPK Instruments), as well as Jezz Leckenby (Talking Science) for the critical review during the preparation of the manuscript. Further assistance from Gabriela Bagordo (JPK Instruments) with the graphic design of the figures is gratefully acknowledged.

References

[1] DJ Muller, *Biochemistry* 47 (2008) 7986–98.
[2] A Berquand et al., *Microscopy Today* 18 (2010) 8–14.
[3] R Tomer et al., *Nat Methods* 9 (2012) 755–63.
[4] T Ando et al., *Proc Natl Acad Sci USA* 98 (2001) 12468–72.
[5] LM Picco et al., *Nanotechnology* 18 (2006) 044030.
[6] MB Viani et al., *Nat Struct Biol* 7 (2000) 644–47.
[7] T Ando, *Nanotechnology* 23 (2012) 062001.
[8] DR Stamov et al., *Ultramicroscopy* 149 (2015) 86–94.
[9] A Monserrate et al., *ChemPhysChem* 15 (2014) 647–50.
[10] L Bozec et al., *Biophys J* 92 (2007) 70–75.
[11] P Rahe et al., *J Vac Sci Technol B* 28 (2010) C4E31.
[12] A Pyne et al., *Small* 10 (2014) 3257–61.
[13] DJ Müller et al., *Biophys J* 68 (1995) 1681–86.
[14] T Ando et al., *Chem Rev* 114 (2014) 3120–88.
[15] HJ Butt et al., *EMBO J* 8 (1989) 1657–63.
[16] J Klingauf et al., *Nature* 394 (1998) 581–85.
[17] SW Schneider et al., *Proc Natl Acad Sci USA* 94 (1997) 316–21.
[18] T Fukuma et al., *Rev Sci Instrum* 77 (2006) 123703.

MT